

How to train your demon to do fast information erasure without heat production

Stephen Whitelam^{✉*}

[✉]*Molecular Foundry, Lawrence Berkeley National Laboratory, 1 Cyclotron Road, Berkeley, CA 94720, USA*

Time-dependent protocols that perform irreversible logical operations, such as memory erasure, cost work and produce heat, placing bounds on the efficiency of computers. Here we use a prototypical computer model of a physical memory to show that it is possible to learn feedback-control protocols to do fast memory erasure without input of work or production of heat. These protocols, which are enacted by a neural-network “demon”, do not violate the second law of thermodynamics because the demon generates more heat than the memory absorbs. The result is a form of nonlocal heat exchange in which one computation is rendered energetically favorable while a compensating one produces heat elsewhere, a tactic that could be used to rationally design the flow of energy within a computer.

I. INTRODUCTION

Landauer’s principle states that erasing a bit of memory at temperature T costs at least $k_B T \ln 2$ units of work and generates the same amount of heat, placing bounds on the efficiency of computing [1–7]. Moreover, these bounds are long-time limits: erasure protocols that occur in finite time t_f cost more energy than the Landauer bound by an amount that increases (to leading order) as $1/t_f$ [8–11]. Thus, for a given physical system, the faster the computation the more heat it is likely to produce.

One way to locally suppress heat production during fast computation is to use fluctuating nanoscale elements controlled by feedback protocols. Such protocols can convert measurement information into stored heat and work [12–19]: Maxwell’s demon, for instance, can create a heat engine by moving a partition in response to the fluctuations of gas molecules. Here we show that feedback protocols can exploit the thermal fluctuations of a model nanoscale memory unit to perform erasure without requiring work or producing heat, even if erasure happens far from equilibrium. Moreover, we show that such protocols can be learned in an autonomous, iterative way, using data accessible in a laboratory experiment. We consider a computer model of an overdamped colloidal particle in a double-well potential, a prototype of a single-bit memory. We use evolutionary methods to train a deep-neural-network demon that can alter the potential in response to input information. When the demon enacts a feedforward protocol, parameterized by time alone, it learns effective and efficient erasure protocols that approach the Landauer bound as the time allotted for erasure is increased. When the demon also receives feedback from the system, the position of the colloidal particle, it can learn erasure protocols that extract work and store heat.

The result is a form of nonlocal heat exchange in which an irreversible computation can be performed in an energetically favorable way, with compensatory heat produced by the measurement apparatus and disposed of

elsewhere. The learning algorithms used in this paper can be applied to experiment, and so the present results suggest a way of designing protocols to do computation with heat moved around a system for convenience.

II. MODEL AND SIMULATION DETAILS

Consider a computer model of a colloidal particle in a potential, sketched in Fig. 1. The particle has position x , and undergoes the Langevin dynamics

$$\dot{x} = -\partial_x U_c(x) + \xi(t), \quad (1)$$

where $\langle \xi(t) \rangle = 0$ and $\langle \xi(t)\xi(t') \rangle = 2\delta(t-t')$. Temperature is held constant throughout the paper, and we express energies in units of $k_B T$. The potential $U_c(x)$ is

$$U_c(x) = c_1 x + c_2 x^2 + c_4 x^4, \quad (2)$$

parameterized by the coefficients $\mathbf{c} = (c_1, c_2, c_4)$. This model defines a 1-bit memory, with its binary state $s = 0, 1$ determined by the location of the particle with respect to the origin, $s = \Theta(x)$ [20]. At times $t = 0$ and $t = t_f$ the potential parameters are $\mathbf{c}_0 = (0, -2w, w)$, and so the potential has the double-well form shown in Fig. 1(a). This has minima at $x = \pm 1$ and barrier height $w = 5 k_B T$. For times $0 < t < t_f$, the parameters \mathbf{c} are determined by a neural network. A neural network can represent an arbitrary function $U(x)$, if we allow full control of the system [21], but here, to make closer contact with experiment, we consider the case of partial control, where only the coefficients \mathbf{c} can be varied. In experiment, similar control can be effected by changing the power of a set of lasers [4].

Dynamical trajectories are run for time t_f . We consider trajectories longer and shorter than the basic relaxation time $t_0 = 2$ of the system. The latter is the characteristic time for the particle, in the absence of a potential, to diffuse a distance equal to that between the potential well centers. (The relation of t_0 to experimental times depends on the details of the experiment: for example, Ref. [4] uses a 200 nm colloidal particle, whose

* swhitelam@lbl.gov

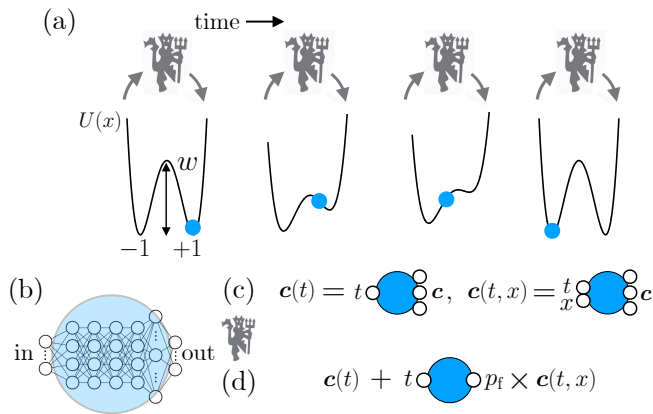


FIG. 1. Memory erasure by a neural-network demon. (a) We consider a particle undergoing Langevin dynamics in a potential $U_c(x)$, Eq. (2), with the state of the memory given by $s = \Theta(x)$. A reset protocol is enacted by a neural-network demon, so that after time t_f the system is in state $s = 0$, regardless of its starting state. The demon controls the three coefficients \mathbf{c} of the potential, similar to experiments that control the output power of a set of lasers. (b) All neural networks used in this paper have the same internal structure. (c) We consider demon protocols parameterized as a function of time; and time and position; and (d) a probabilistic combination of both.

diffusion constant is $D \sim (\mu\text{m})^2/\text{s}$, and a well-to-well separation of $2.5 \mu\text{m}$, giving t_0 of order 10 seconds.)

At time $t = 0$ the position x_0 of the particle is drawn from the Boltzmann distribution $\rho_0(x_0, \mathbf{c}_0) = e^{-U_{\mathbf{c}_0}(x_0)} / \int dx' e^{-U_{\mathbf{c}_0}(x')}$. Let $k = 1, 2, \dots, K = \lfloor t_f/\Delta t \rfloor$ label the simulation step. At regular time intervals $\Delta t = 10^{-3}$ the potential coefficients are set to new values, $\mathbf{c}_k \rightarrow \mathbf{c}_{k+1}$, and the change of work recorded, $\Delta W_k = U_{\mathbf{c}_{k+1}}(x_k) - U_{\mathbf{c}_k}(x_k)$. The position of the particle is updated according to the forward Euler discretization of (1),

$$x_{k+1} = x_k - \Delta t \partial_x U_{\mathbf{c}_{k+1}}(x) + \sqrt{2\Delta t} \xi, \quad (3)$$

where $\xi \sim \mathcal{N}(0, 1)$, and the change of heat recorded, $\Delta Q_k = U_{\mathbf{c}_{k+1}}(x_{k+1}) - U_{\mathbf{c}_{k+1}}(x_k)$. The total work and heat are $W = \sum_{k=0}^{K-1} \Delta W_k$ and $Q = \sum_{k=0}^{K-1} \Delta Q_k$. Note that $\mathbf{c}_K = \mathbf{c}_0$ and $W + Q = U_{\mathbf{c}_0}(x_K) - U_{\mathbf{c}_0}(x_0)$.

When the potential coefficients are updated, they are set to the values $\mathbf{c} = \mathbf{g}_\theta(\mathbf{i})$, determined by a deep neural network. Here \mathbf{g} is the output 3-vector of the neural network, \mathbf{i} is the input vector provided to the neural network, and θ is the vector of neural-network parameters (weights and biases). Details of the neural network are given in the attached code [22]. Briefly, it has an internal structure that is fully connected, with 4 hidden layers of width 4 and a final hidden layer of width 10, indicated by the blue circle in Fig. 1(b). Neurons have tanh nonlinearities, and layer norm is used. This network structure is expressive enough to learn a range of functions, including rapidly-varying ones, and straightforward to train using

non-gradient algorithms [23]. The arguments \mathbf{i} are the inputs of the neural network. As sketched in Fig. 1(c), we consider feedforward protocols $\mathbf{c}(t) = (c_1(t), c_2(t), c_4(t))$ parameterized by time alone, in which case $\mathbf{i} = t/t_0$, and feedback protocols $\mathbf{c}(t, x) = (c_1(t, x), c_2(t, x), c_4(t, x))$ parameterized by time and particle position, in which case $\mathbf{i} = (t/t_0, x)$. The network has as many input neurons as input degrees of freedom.

In an effort to learn protocols that achieve a particular objective, we use a genetic algorithm [24–27] to adjust the parameters θ of the neural network. This procedure is described in Ref. [28], and details are given in the attached code [22]. Briefly, we consider a population of 50 neural-network demons, each characterized by a value ϕ that is calculated by averaging a chosen quantity (see below) over 10^4 independent trajectories. At the start of the evolutionary process, demon parameters are set equal to random numbers. The 5 demons with the smallest values of ϕ are chosen to be the parents of subsequent generations. These 5 are cloned and mutated, by adding random numbers to their parameters, to produce another population of 50. The procedure is repeated for several generations, the intent being to produce neural-network demons whose protocols give rise to values of ϕ as small as possible. For reversible protocols (particle translation and bit flipping) parameterized by time, this procedure recovers optimal-control results obtained analytically and by other numerical approaches [28–30]. In this paper we apply these methods to the irreversible operation of memory erasure. In Fig. A1 we benchmark the learning algorithm on a driven barrier-crossing problem closely related to the problem considered in the main text, showing that it reproduces the optimal-control protocols of Ref. [31].

III. LEARNING EFFECTIVE AND EFFICIENT ERASURE PROTOCOLS

We first apply the evolutionary procedure to a feedforward protocol $\mathbf{c}(t)$, which is parameterized by time alone. We choose to minimize the objective function

$$\phi = 1 - P_0 + k_w \langle W \rangle, \quad (4)$$

where $P_0 \equiv \langle \Theta(-x(t_f)) \rangle$ is the mean probability of reset. Here $\langle \cdot \rangle$ denotes the mean over 10^4 independent trajectories. Minimizing the term $1 - P_0$ encourages protocols that reset the memory. Minimizing the final term in (4) minimizes the mean work done under the protocol. The factor $k_w = 0.05$ ensures that the final term in (4) is smaller than $1 - P_0$ until the probability of reset gets close to one, ensuring that the first goal of the evolutionary process is to produce a reset protocol, and the second goal is to do so with as little work as possible.

Fig. 2 shows the results of this procedure, for trajectory lengths $t_f = 1, 10, \text{ and } 100$. As shown in panel (a), all result in protocols that achieve reset (with probability $\gtrsim 99.8\%$) after sufficient evolutionary generations. These

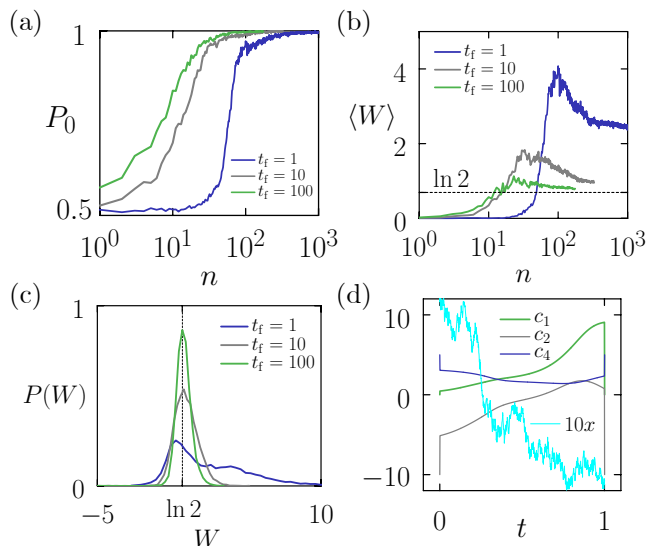


FIG. 2. Evolutionary learning of feedforward erasure protocols parameterized by time, $c(t)$. (a) Mean probability of erasure, P_0 , for the best-performing protocol of generation n , for three different trajectory lengths t_f . Averages are taken over 10^4 trajectories. (b) Mean work $\langle W \rangle$ for the best-performing protocol of generation n . (c) Histograms $P(W)$ of work done for the best-performing protocol from the latest generation achieved for each t_f (generations 1208, 327, and 175, for $t_f = 1, 10$, and 100, respectively). In (b) and (c), the dotted line is the Landauer bound. (d) Erasure protocol $c(t)$ for $t_f = 1$ learned after 1208 evolutionary generations. The cyan line shows the trajectory of a single particle under this protocol.

choices of t_f correspond to a range from short to long, relative to the system's basic diffusive timescale $t_0 = 2$, and so present different challenges. Trajectories of length t_f less than t_0 must involve strong driving, in order to move the particle the required distance in the allotted time. Gentler driving suffices for trajectories much longer than t_0 , but effective reset protocols must still have a nonequilibrium character: the memory is volatile in the sense that the default energy barrier of $5 k_B T$ can be readily surmounted by thermal fluctuations, and so energy input is required in order to maintain the fidelity of the memory. Assuming an escape time of $t_e \approx \exp(5) \approx 150$, and modeling the potential as a 2-level system, memories that achieve reset and are then left in their final form for time t_f have a probability of remaining reset of approximately $(1 + e^{-2t/t_e})/2$, which is only $\approx 94\%$ or $\approx 63\%$ for $t_f = 10$ or $t_f = 100$, respectively. The learned protocols are considerably more effective.

Fig. 2(b) shows that the mean work $\langle W \rangle$ required to achieve reset is close to the Landauer bound for $t_f = 100$, and over $k_B T$ away from the bound for $t_f = 1$. These results are consistent with experiments done for times t_f larger and smaller than the system's basic relaxation time t_0 [4]. Also consistent with those experiments, the work distribution resulting from the best protocol for each t_f becomes increasingly sharply peaked about the

Landauer bound as t_f increases: see panel (c). Individual trajectories can achieve work values that violate the bound and even store work [32–35]. Panel (d) shows one of the learned time-dependent protocols, which is non-monotonic and displays jumps in the values of the potential coefficients at the start and end of the trajectory. Nonmonotonic features [31] and jumps [29, 36] are present in optimal-control protocols for other systems.

Fig. 3 illustrates the near-equilibrium and far-from-equilibrium character of the learned reset procedure for the cases $t_f = 10$ and 1, respectively. For $t_f = 10$, histograms of particle position $\rho(x)$ are, for most of the trajectory, close to the Boltzmann distribution $\rho_0(x, c)$ associated with the instantaneous potential $U_c(x)$. At the end of the trajectory, these things become distinct: the particle-position histogram is consistent with a reset probability close to 1, while the Boltzmann distribution is consistent with a reset probability of 1/2. For the case $t_f = 1$, particle-position histograms and Boltzmann distributions are clearly different for most of the trajectory. Reset happens in a far-from-equilibrium way, requiring energy expenditure considerably in excess of the Landauer bound.

IV. FEEDBACK PROTOCOLS

In this section we consider feedback protocols $c(t, x)$ that are parameterized as a function of time t and particle position x . Such protocols can be used to do fast erasure while violating the Landauer bound, if only the memory unit is considered. The cost of this violation is paid for by the acquisition (and subsequent erasure) of the particle coordinates, and so, in effect, one erasure process is used to control another erasure process. The advantage of doing so is that it is possible to render the chosen process energy efficient; the cost is that the controlling protocol is relatively inefficient. We shall also consider the question of how to learn probabilistic feedback-feedforward protocols that perform erasure with specified accuracy and efficiency, while making as few measurements as possible.

In Fig. 6(a,b) we show that evolutionary learning applied to a demon fed both time t and particle position x can again produce effective protocols, with reset probabilities in excess of 99.9%. Moreover, the mean work done upon reset is negative, with about $40 k_B T$ extracted from the thermal bath in which the colloidal particle is immersed, even through the trajectory is short ($t_f = 1$) relative to the basic diffusion time $t_0 = 2$. A similar amount of heat is absorbed from the bath. Fig. 4 compares feedback protocols and feedforward (time-parameterized) protocols, showing that the former extract work from the bath through the small changes the demon makes to the potential coefficients in response to fluctuations of particle position. Panel (c) shows the behavior of the potential coefficients for a single feedback-controlled trajectory in which the particle started in state $s = 1$. Fig. 5 illustrates the shape of the potential as a function of time. (For the

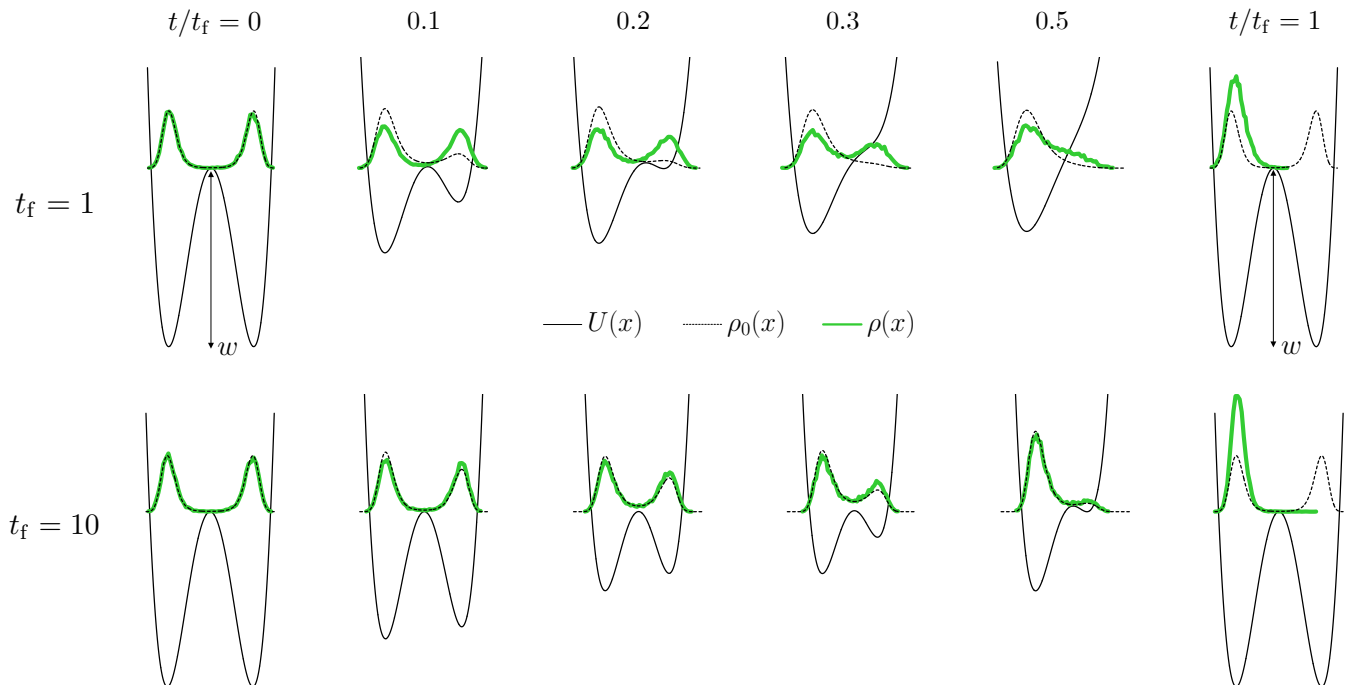


FIG. 3. Potentials $U(x)$ (black) and associated Boltzmann distributions $\rho_0(x)$ (dashed black) at 6 values of scaled time t/t_f , under feedforward protocols $\mathbf{c}(t)$ learned (after 1208 or 327 generations, respectively) by evolution for trajectory lengths $t_f = 1$ (top) and $t_f = 10$ (bottom). Histograms $\rho(x)$ of particle positions for 10^4 independent trajectories are shown in green. The scale of the potential is set by the well depth $w = 5k_B T$ at times $t = 0, t_f$, and by the fact that the potential minima are at $x = \pm 1$. The common scale of the histograms and Boltzmann distributions is set by the Boltzmann distribution of $U(x)$ at times $t = 0, t_f$, and by the fact that the area under each histogram is unity.

feedback protocol, the time evolution of the potential is different when the particle starts instead in state $s = 0$: in that case, the potential minima fluctuate a little in order to extract work from the particle, but the potential shape does not change substantially.)

Thus a feedback protocol can perform an irreversible logical operation in such a way that the surrounding thermal bath is cooled, rather than heated. To compensate, the demon must receive (and then erase) the real-valued colloidal coordinates it uses to perform the protocol. Assuming that each coordinate is represented as a 32-bit floating-point number, the demon requires at least $32k_B T \ln 2$ units of work to erase each measurement. For a trajectory of length $t_f = 1$, the demon makes 10^3 measurements, and so consumes at least 32,000 $k_B T \ln 2$ units of work. With about $40k_B T$ stored in the memory, the efficiency of the system is then about 0.2%. The demon-memory system is therefore inefficient, but effective in the sense that the designated computation is done in an energetically favorable way, with waste heat sent elsewhere.

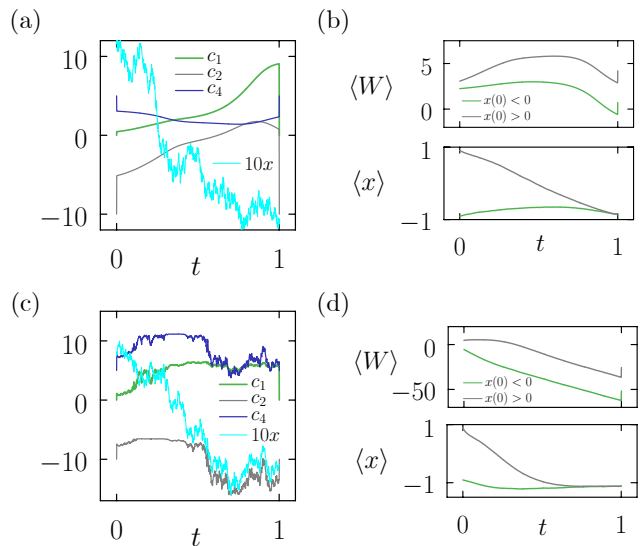


FIG. 4. Comparison of feedforward- (top) and feedback- (bottom) erasure protocols produced by evolutionary learning. Panel (a) is Fig. 2(d), and panel (c) is its counterpart for a feedback protocol. Panels (b) and (d) show the mean work and mean position of particles under these protocols, separated according to whether the particle started in state $s = 0$ (green) or $s = 1$ (gray).

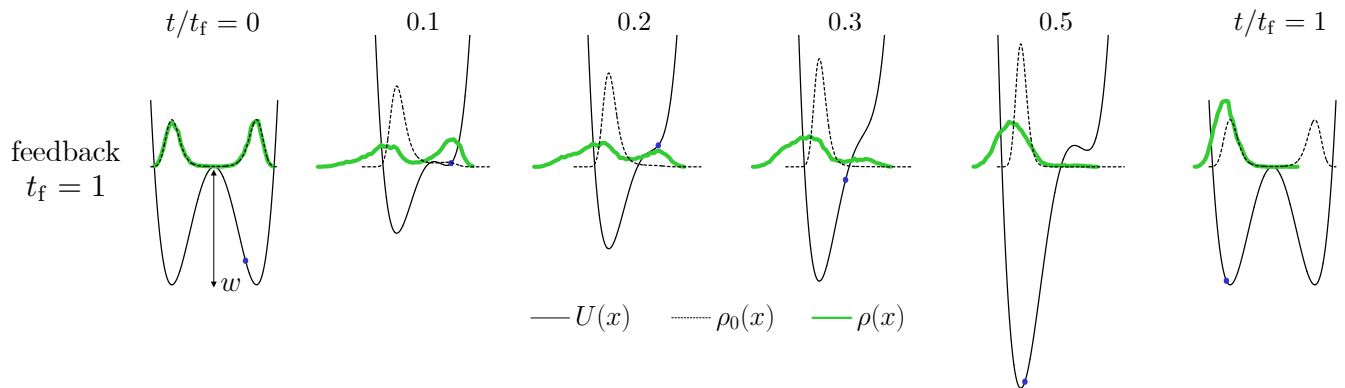


FIG. 5. Similar to Fig. 3, but now for an evolution-learned feedback protocol $\mathbf{c}(t, x)$. With feedback, the potential $U(x)$ is different for each trajectory. We show the potential (black) from a trajectory in which the particle started in state $s = 1$ (the instantaneous position of the particle is shown by a blue dot), and the associated Boltzmann distribution (black dashed) for that potential. Histograms $\rho(x)$ of particle positions for 10^4 independent trajectories (starting with equal probability from either state) are shown green.

V. PROBABILISTIC FEEDBACK-FEEDFORWARD PROTOCOLS

One way to reduce the information cost of a feedback protocol is to allow the demon to choose when to make measurements. To do so, we can impose an evolutionary order parameter ϕ that encourages measurements to be made only when necessary, and allow the demon to choose, probabilistically, when to measure the particle coordinate x . This idea is sketched in Fig. 1(d). (The cost of measurement has also been considered in gradient-based approaches to reinforcement learning [37], and the choice of stochastic versus deterministic control of a system has been explored in Ref. [38].) When the demon acts, it sets the potential coefficients \mathbf{c} to the values

$$\mathbf{c} = \begin{cases} \mathbf{g}_{\theta_1}(t) & (\xi \geq p_f(t)) \\ \mathbf{g}_{\theta_1}(t) + \mathbf{g}_{\theta_2}(t, x) & (\xi < p_f(t)). \end{cases} \quad (5)$$

Here $\mathbf{g}_{\theta_1}(t)$ and $\mathbf{g}_{\theta_2}(t, x)$ are neural networks whose structures are shown in Fig. 1(b,c): each has three outputs, specifying the values of the potential coefficients \mathbf{c} , and a number of inputs equal to the number of input parameters it is fed (one for the case of the feedforward protocol $\mathbf{g}_{\theta_1}(t)$, and two for the case of the feedback protocol $\mathbf{g}_{\theta_2}(t, x)$). ξ is a uniform random real number on $(0, 1]$, and $p_f(t) = \mathbf{g}_{\theta_3}(t) \in [0, 1]$ is the output of a third neural network (this has one input node, which accepts time t , and one output node, which specifies the probability p_f). Thus at time t the demon decides with probability p_f to measure the particle position x and update the potential coefficients using a feedback protocol. With probability $1 - p_f$ the demon makes no measurement, and instead updates \mathbf{c} using a feedforward protocol.

We instruct the learning algorithm to minimize the

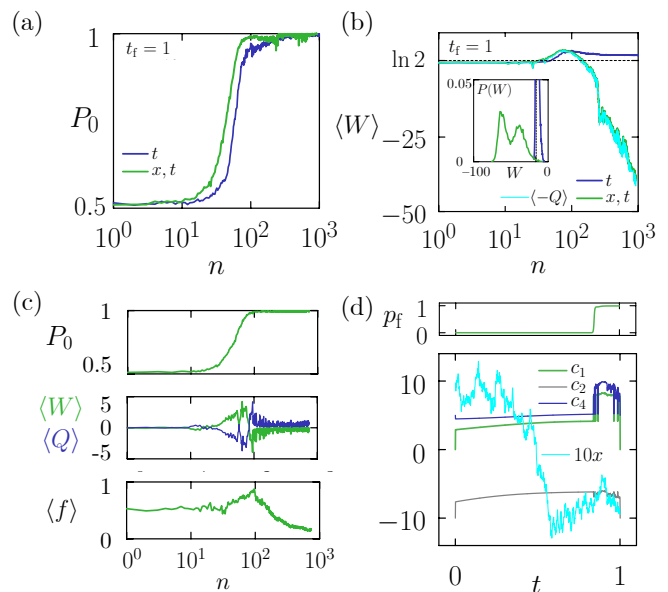


FIG. 6. Feedback erasure protocols produced by evolutionary learning. Panels (a) and (b) are similar to those of Fig. 2, and include the time-dependent protocol for the case $t_f = 1$ (blue, labeled “ t ”), together with results obtained by training a feedback protocol $\mathbf{c}(t, x)$ (green, labeled “ x, t ”). The mean heat exchanged by the feedback protocol is shown in cyan: positive values of Q indicate heat adsorption (negative entropy production). The inset to (b) shows the work distribution under the protocol learned after 922 generations (green), compared with that learned under the feedforward protocol of Fig. 2 (blue). (c) Results obtained using a probabilistic feedback protocol (5) in which the demon can decide whether or not to make a measurement; f is the number of measurements it makes, divided by the maximum possible number of measurements. (d) Trajectory produced using the best performing protocol from generation 722 of (c): p_f is the probability with which the demon makes a measurement.

evolutionary order parameter

$$\phi = \begin{cases} k_n \langle n_f \rangle & (P_0 > 0.99 \text{ and } \langle W \rangle < 0) \\ 1 - P_0 + k_w \langle W \rangle + k_c & (\text{otherwise}), \end{cases} \quad (6)$$

where $k_n = 3 \times 10^{-4}$, $k_w = 0.05$, and $k_c = 20$ are constants. Here n_f is the number of measurements of particle position made by the demon within a trajectory. The motivation behind Eq. (6) is to imagine that we have a strict engineering requirement for a protocol with certain properties, such as to achieve reset with at least 99% probability without energy expenditure, and then to ask for this to happen using as few measurements as possible (an alternative approach would be to consider the Pareto frontiers for combinations of these quantities). The second clause in (6) is (4) shifted by a constant, and asks the demon to learn a reset protocol that requires as little work as possible. When it has produced a protocol with probability of reset $P_0 > 0.99$ that does not consume work, the first clause in (6) becomes active and asks the demon to make as few measurements as possible. The constants k ensure that the first clause in (6) is always numerically smaller than the second – as long as this is achieved, the precise numerical values of the constants are not important – and so minimizing ϕ encourages the demon to maintain $P_0 \approx 0.99$ and $\langle W \rangle \approx 0$ while making as few measurements as possible.

The results of this learning procedure are shown in Fig. 6(c). As a function of evolutionary time n , the demon first learns to produce a reset protocol, and then to do so with no work consumed (and no heat expended, because $W \approx -Q$). During this stage of evolution it makes measurements more frequently in order to reduce the work done during reset. Subsequently, it learns to maintain a reset protocol with $P_0 \approx 0.99$ and $\langle W \rangle \approx 0$ while making fewer measurements. In this phase it learns to make a fraction $f \approx 15\%$ of the measurements it would have made in a pure feedback protocol. Fig. 6(d) shows that its strategy for doing so is strongly time-dependent. For the majority of the trajectory the demon maintains the measurement-feedback probability p_f close to zero, and enacts a feedforward protocol. Close to the end of the trajectory it sets p_f close to one, and makes frequent measurement-feedback decisions in order to make the reset process energetically neutral.

VI. CONCLUSIONS

We have shown that evolutionary methods can train a deep-neural-network demon to identify reset protocols for a noisy and volatile memory element, on timescales longer and shorter than its basic relaxation time. These protocols are effective, achieving reset with probability

close to one, and are energy-efficient, approaching the Landauer bound as protocol time is increased. For times short compared to the basic relaxation time of the system, reset requires work considerably in excess of the Landauer bound, consistent with experiments. In this short-time regime, we have shown that feedback protocols can effect reset without heat production. In this mode the demon performs nonlocal heat exchange, generating heat and doing work by making measurements and deleting data, while the memory element under its control produces no heat or stores it.

The evolutionary learning method used to train the demon is technically simple and effective. It reproduces optimal-control results obtained by other methods, for feedforward protocols parameterized by time alone, and can identify feedback protocols that satisfy multiple objectives of fidelity and efficiency. Given that it takes as input time- and ensemble averages of fluctuating quantities that are accessible experimentally, the present results suggest a way of designing experimental protocols that do computation with heat moved around a system for convenience.

VII. ACKNOWLEDGMENTS

I thank Adrienne Zhong for providing the data from Ref. [31] labeled “OCT” in Fig. A1, and thank Corneel Casert and Isaac Tamblyn for discussions. Code for doing evolutionary learning of a feedback erasure protocol can be found at Ref. [22]. This work was performed at the Molecular Foundry at Lawrence Berkeley National Laboratory, supported by the Office of Basic Energy Sciences of the U.S. Department of Energy under Contract No. DE-AC02-05CH11231.

Appendix A: Benchmarking the evolutionary learning algorithm

In Fig. A1 we benchmark the evolutionary learning algorithm on the driven barrier-crossing problem of Ref. [31]; see panels (b) and (d) of Fig. 2 of that paper. A particle undergoes the Langevin dynamics (1), with $U_c(x)$ replaced by the the potential $U_\lambda(x) = 16[(x^2 - 1)^2/4 - \lambda x]$, in units of $k_B T$. The initial and final values of the control parameter λ are $\lambda(0) = -1$ and $\lambda(t_f) = 1$, and we train a neural network to express $\lambda(t)$ for $0 < t < t_f$ so as to minimize $\phi = \langle W \rangle$. Each particle begins in equilibrium in the left-hand potential well, and averages are calculated over 10^4 independent trajectories. Our results are consistent with the optimal-control solutions of Ref. [31].

[1] Rolf Landauer, “Irreversibility and heat generation in the computing process,” IBM journal of research and devel-

opment **5**, 183–191 (1961).

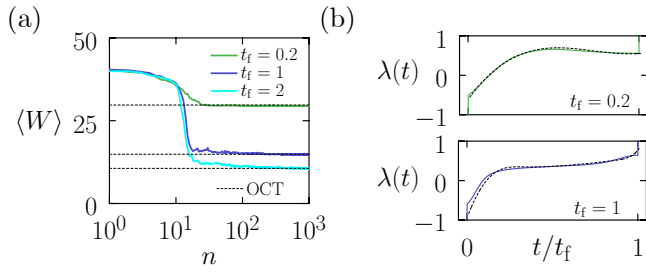


FIG. A1. Benchmarking the learning algorithm using the driven barrier-crossing problem of Ref. [31]. (a) $\langle W \rangle$ for the best-performing protocol as a function of evolutionary time n , for three values of t_f (colors); these converge to the values calculated by the optimal control theory (OCT) approach of Ref. [31] (dashed black). (b) Learned protocols as a function of time for two values of t_f . These converge to forms that fluctuate (with increasing generation) about the noise-free OCT solutions (dashed black). For $t_f = 0.2$ the profile is nonmonotonic, consistent with the results of Ref. [31].

- [2] Barbara Piechocinska, “Information erasure,” *Physical Review A* **61**, 062314 (2000).
- [3] Raoul Dillenschneider and Eric Lutz, “Memory erasure in small systems,” *Physical Review Letters* **102**, 210601 (2009).
- [4] Yonggun Jun, Momčilo Gavrilov, and John Bechhoefer, “High-precision test of Landauer’s principle in a feedback trap,” *Physical Review Letters* **113**, 190601 (2014).
- [5] Antoine Bérut, Artak Arakelyan, Artyom Petrosyan, Sergio Ciliberto, Raoul Dillenschneider, and Eric Lutz, “Experimental verification of Landauer’s principle linking information and thermodynamics,” *Nature* **483**, 187–189 (2012).
- [6] Salambô Dago, Jorge Pereda, Nicolas Barros, Sergio Ciliberto, and Ludovic Bellon, “Information and thermodynamics: fast and precise approach to Landauer’s bound in an underdamped micromechanical oscillator,” *Physical Review Letters* **126**, 170601 (2021).
- [7] Jeongmin Hong, Brian Lambson, Scott Dhuey, and Jeffrey Bokor, “Experimental test of Landauer’s principle in single-bit operations on nanomagnetic memory bits,” *Science advances* **2**, e1501492 (2016).
- [8] Karel Proesmans, Jannik Ehrich, and John Bechhoefer, “Finite-time Landauer principle,” *Physical Review Letters* **125**, 100602 (2020).
- [9] Patrick R Zulkowski and Michael R DeWeese, “Optimal finite-time erasure of a classical bit,” *Physical Review E* **89**, 052140 (2014).
- [10] Salambô Dago and Ludovic Bellon, “Dynamics of information erasure and extension of Landauer’s bound to fast processes,” *Physical Review Letters* **128**, 070604 (2022).
- [11] Michael Konopik, Till Korten, Eric Lutz, and Heiner Linke, “Fundamental energy cost of finite-time parallelizable computing,” *Nature Communications* **14**, 447 (2023).
- [12] Leo Szilard, “On the decrease of entropy in a thermodynamic system by the intervention of intelligent beings,” *Behavioral Science* **9**, 301–310 (1964).
- [13] Takahiro Sagawa and Masahito Ueda, “Nonequilibrium thermodynamics of feedback control,” *Physical Review E* **85**, 021104 (2012).
- [14] Massimiliano Esposito and Gernot Schaller, “Stochastic thermodynamics for “Maxwell demon” feedbacks,” *EPL (Europhysics Letters)* **99**, 30003 (2012).
- [15] Juan MR Parrondo, Jordan M Horowitz, and Takahiro Sagawa, “Thermodynamics of information,” *Nature physics* **11**, 131–139 (2015).
- [16] Jannik Ehrich, Susanne Still, and David A Sivak, “Energetic cost of feedback control,” *arXiv preprint arXiv:2206.10793* (2022).
- [17] Giovanni Diana, G Baris Bagci, and Massimiliano Esposito, “Finite-time erasing of information stored in fermionic bits,” *Physical Review E* **87**, 012111 (2013).
- [18] Shoichi Toyabe, Takahiro Sagawa, Masahito Ueda, Eiro Muneyuki, and Masaki Sano, “Experimental demonstration of information-to-energy conversion and validation of the generalized Jarzynski equality,” *Nature physics* **6**, 988–992 (2010).
- [19] David Abreu and Udo Seifert, “Extracting work from a single heat bath through feedback,” *Europhysics Letters* **94**, 10001 (2011).
- [20] We define $\Theta(x) = 1$ if $x \geq 0$ and $\Theta(x) = 0$ otherwise.
- [21] Karel Proesmans, Jannik Ehrich, and John Bechhoefer, “Optimal finite-time bit erasure under full control,” *Physical Review E* **102**, 032105 (2020).
- [22] <https://github.com/swhitelam/erasure>.
- [23] Stephen Whitelam, Viktor Selin, Ian Benlolo, Corneel Casert, and Isaac Tamblin, “Training neural networks using Metropolis Monte Carlo and an adaptive variant,” *Machine Learning: Science and Technology* **3**, 045026 (2022).
- [24] John H Holland, “Genetic algorithms,” *Scientific American* **267**, 66–73 (1992).
- [25] Melanie Mitchell, *An introduction to genetic algorithms* (MIT press, 1998).
- [26] David J Montana and Lawrence Davis, “Training feed-forward neural networks using genetic algorithms.” in *IJ-CAI*, Vol. 89 (1989) pp. 762–767.
- [27] Felipe Petroski Such, Vashisht Madhavan, Edoardo Conti, Joel Lehman, Kenneth O Stanley, and Jeff Clune, “Deep neuroevolution: genetic algorithms are a competitive alternative for training deep neural networks for reinforcement learning,” *arXiv preprint arXiv:1712.06567* (2017).
- [28] Stephen Whitelam, “Demon in the machine: learning to extract work and absorb entropy from fluctuating nanosystems,” *Physical Review X* **13**, 021005 (2023).
- [29] Tim Schmiedl and Udo Seifert, “Optimal finite-time processes in stochastic thermodynamics,” *Physical Review Letters* **98**, 108301 (2007).
- [30] Megan C Engel, Jamie A Smith, and Michael P Brenner, “Optimal control of nonequilibrium systems through automatic differentiation,” *arXiv preprint arXiv:2201.00098* (2022).
- [31] Adrienne Zhong and Michael R DeWeese, “Limited-control optimal protocols arbitrarily far from equilibrium,” *Physical Review E* **106**, 044135 (2022).
- [32] Christopher Jarzynski, “Nonequilibrium equality for free energy differences,” *Physical Review Letters* **78**, 2690 (1997).
- [33] Denis J Evans and Debra J Searles, “The fluctuation theorem,” *Advances in Physics* **51**, 1529–1585 (2002).
- [34] Gavin E Crooks, “Entropy production fluctuation theorem and the nonequilibrium work relation for free energy

- differences,” *Physical Review E* **60**, 2721 (1999).
- [35] Udo Seifert, “Stochastic thermodynamics, fluctuation theorems and molecular machines,” *Reports on Progress in Physics* **75**, 126001 (2012).
- [36] Steven Blaber, Miranda D Louwerse, and David A Sivak, “Steps minimize dissipation in rapidly driven stochastic systems,” *Physical Review E* **104**, L022101 (2021).
- [37] Colin Bellinger, Andriy Drozdyuk, Mark Crowley, and Isaac Tamblyn, “Balancing information with observation costs in deep reinforcement learning,” in *Proceedings of the 35th Canadian Conference on Artificial Intelligence. CAIAC* (2022).
- [38] Hilbert J Kappen, “Linear theory for control of nonlinear stochastic systems,” *Physical Review Letters* **95**, 200201 (2005).